Lattice instabilities in bulk $EuTiO_3$

D. Bessas,[1,2,*] K. Z. Rushchanskii,[3] M. Kachlik,[4] S. Disch,[1,5] O. Gourdon,[6,7,†] J. Bednarcik,[8] K. Maca,[4] I. Sergueev,[1,9,‡] S. Kamba,[10] M. Ležaić,[3] and R. P. Hermann[1,2,§]

[1]*Jülich Centre for Neutron Science JCNS and Peter Grünberg Institut PGI, JARA-FIT, Forschungszentrum Jülich GmbH, D-52425 Jülich, Germany*

[2]*Faculté des Sciences, Université de Liège, B-4000 Liège, Belgium*

[3]*Peter Grünberg Institut, Quanten-Theorie der Materialien, Forschungszentrum Jülich and JARA, D-52425 Jülich, Germany*

[4]*CEITEC Brno University of Technology, 61600 Brno, Czech Republic*

[5]*Institut Laue-Langevin, F-38042 Grenoble, France*

[6]*Neutron Scattering Science Division, Oak Ridge National Laboratory, Oak Ridge, Tennessee 37831, USA*

[7]*Jülich Centre for Neutron Science JCNS, Oak Ridge National Laboratory, Oak Ridge, Tennessee 37831, USA*

[8]*Deutsches Electronen-Synchrotron, D-22607 Hamburg, Germany*

[9]*European Synchrotron Radiation Facility, F-38043 Grenoble, France*

[10]*Institute of Physics ASCR, 18221 Prague, Czech Republic*

(Received 28 August 2012; revised manuscript received 2 October 2013; published 28 October 2013)

The phase purity and the lattice dynamics in bulk $EuTiO_3$ were investigated both microscopically, using x-ray and neutron diffraction, ^{151}Eu-Mössbauer spectroscopy, and ^{151}Eu nuclear inelastic scattering, and macroscopically using calorimetry, resonant ultrasound spectroscopy, and magnetometry. Furthermore, our investigations were corroborated by *ab initio* theoretical studies. The perovskite symmetry, $Pm\bar{3}m$, is unstable at the M- and R-points of the Brillouin zone. The lattice instabilities are lifted when the structure relaxes in one of the symmetries: $I4/mcm$, $Imma$, $R\bar{3}c$ with relative relaxation energy around -25 meV. Intimate phase analysis confirmed phase purity of our ceramics. A prominent peak in the Eu specific density of phonon states at 11.5 meV can be modeled in all candidate symmetries. A stiffening on heating around room temperature is indicative of a phase transition similar to the one observed in $SrTiO_3$, however, although previous studies reported the structural phase transition to the tetragonal $I4/mcm$ phase our detailed sample purity analysis and thorough structural studies using complementary techniques did not confirm a direct phase transition. Instead, in the same temperature range, Eu delocalization is observed which might explain the lattice dynamical instabilities.

DOI: 10.1103/PhysRevB.88.144308 PACS number(s): 63.20.dd, 61.05.C−, 62.20.D−, 76.80.+y

I. INTRODUCTION

Perovskites exhibit cubic symmetry at high temperature, with space group $Pm\bar{3}m$ and a large flexibility of site occupancy by a broad range of elements on the A and B sites[1] and flexibility in oxygen stoichiometry on the X site,[2] indicated in the general chemical formula $ABX_{3\pm\delta}$. The oxygen in the perovskite unit cell form interconnected octahedra, the rotation of which are potentially responsible for distortions away from the cubic symmetry and structural transitions.[3] Ba, Sr, and, to a lesser extent, Eu perovskite titanates are interesting owing to their ferroelectric properties and their potential applications in information technology. $EuTiO_3$ is an incipient ferroelectric perovskite, like $SrTiO_3$, with, however, magnetic cations on the A site and it undergoes a transition to a G-type antiferromagnetic phase below 5.3 K.[4,5] Recently, ferroelectric instability in $EuTiO_3$ films[6] under 1% tensile stress was reported. However, in bulk $EuTiO_3$ the cubic $Pm\bar{3}m$ structure was until recently supposed to be stable down to liquid-helium temperature.[7] Only lately some hints of an antiferrodistortive phase transition to a tetragonal $I4/mcm$ phase were observed, but the critical temperature varied from 200 to 282 K.[8–11] These results were consistently checked by Goian *et al.*[12] and attributed to the sample quality.

Inelastic x-ray scattering on tiny single crystals was only very recently reported[13] and shows that the antiferrodistortive phase transition cannot be of order-disorder type, as was proposed by Bussmann-Holder *et al.*,[8,14] but is instead displacive with a soft mode at the R point of the Brillouin zone. However, similar zone-boundary phonon softening has been identified without the observation of a structural phase transition by Swainson *et al.*,[15] e.g., in relaxors.

In this study we present a detailed investigation of the phase purity, the crystallinity, and the lattice dynamics in bulk polycrystalline $EuTiO_3$ using both microscopic and macroscopic measurements as well as theoretical calculations. We demonstrate that a lattice instability associated with Eu anharmonic displacements appears close to room temperature.

II. METHODS

A. Experimental techniques

Phase pure $EuTiO_3$ polycrystalline samples were prepared using a stoichiometric ratio of precursors (Eu_2O_3 99.99% and Ti_2O_3 99.9%). The mixture was homogenized in a planetary ball mill, cold isostatically pressed at 300 MPa, and sintered in pure hydrogen at 1400 °C for 2 h. The processing details are given elsewhere.[16] The sintered pellets had a relative density of 89%. All measurements were performed on ceramic pieces or powder taken from the same pellet.

The crystallographic phase purity and potential structural transitions were checked by temperature-dependent powder diffraction between 10 and 300 K using high-energy synchrotron radiation, wavelength 0.142 013 Å, at station 6-ID-D/APS. In order to extend the temperature range up to

400 K similar measurements were carried out with 0.20727 Å wavelength on the same sample at station P02.1/PETRAIII. The overall precision including sample size and detector pixel size was estimated using standard samples to $\Delta d/d \sim 5.0 \times 10^{-3}$ for measurements carried out at 6-ID-D and $\Delta d/d \sim 1.0 \times 10^{-2}$ for measurements carried out at P02.1. The atomic behavior in $EuTiO_3$ was further studied by neutron diffraction. Europium is a strong neutron absorber,[17] thus a thin homogeneous powder layer was prepared using 700 mg of $EuTiO_3$ and placed between thin vanadium foils ($0.02 \times 10 \times 30\,mm^3$). Neutron-scattering data were collected between 150 and 350 K using the time-of-flight (TOF) instrument POWGEN,[18] with precision $\Delta d/d \sim 1.5 \times 10^{-3}$ at $d = 1$ Å, and between 10 and 300 K using the TOF instrument NOMAD[19] at the Spallation Neutron Source. The neutron pair-distribution function (PDF) analysis was carried out on the data obtained at NOMAD by Fourier transformation of the total scattering function.[20]

The phase purity was further investigated using ^{151}Eu-Mössbauer spectroscopy between 90 and 325 K on fine powder of $EuTiO_3$, 35 mg/cm^2, mixed with BN, using a calibrated spectrometer.

Heat-capacity measurements were recorded in the Quantum Design-Physical Properties Measurement System (QD-PPMS) utilizing the built-in calorimeter. Measurements of both the addenda and sample were performed at the same temperatures between 10 and 340 K with a 0.5 K point density in the region of interest. Every data point was measured three times and an average value was extracted.

The macroscopic lattice dynamics was probed by resonant ultrasound spectroscopy (RUS).[21] Temperature-dependent spectra between 100 kHz and a few MHz were recorded on a shaped sample ($2.5 \times 2 \times 1.5\,mm^3$) using an in-house spectrometer made with cylindrical Y-cut $LiNbO_3$ 0.3-mm-thick transducers (Ø 1.5 mm) inside a QD-PPMS.

Magnetic characterizations were carried out in a Cryogenics Ltd. measurement system using ac susceptibility measurements below 30 K ($f = 20.4$ Hz, $H_{ac} = 10$ G at $H_{dc} = 0$ G) as well as dc susceptibility measurements ($H_{dc}^{max} = 5$ kG, at $T = 4.9$ K).

To support our macroscopical lattice dynamical characterization microscopic investigations based on nuclear inelastic scattering (NIS)[22] of ^{151}Eu in $EuTiO_3$ were performed. Several spectra were recorded at 110, 210, 295, and 360 K in 16-bunch mode at the nuclear resonance station ID22N/ESRF[23] using a nested monochromator[24] providing 1.5-meV resolution.

B. Theoretical techniques

The Eu specific density of phonon states, i.e., the spectral distribution of the Eu vibrational amplitude, for $I4/mcm$, $Imma$, and $R\bar{3}c$ structures were calculated using the PHON code[25] by integrating the eigenvectors and eigenvalues of the corresponding dynamical matrices over the Brillouin zone. We used a $30 \times 30 \times 30$ q-point mesh and the experimental full width at half maximum (FWHM) for Gaussian convolution. Details on the calculation of the dynamical matrices as well as the crystallographic parameters of the used structures are given in Ref. 26.

III. RESULTS

A. Microscopic characterization

A typical x-ray diffractogram recorded on polycrystalline $EuTiO_3$ is shown in Fig. 1(a). The Q range of our scattering data reached approximately 13 Å^{-1} using neutrons. A typical TOF neutron diffractogram is given in Fig. 1(c). All observed reflections were identified in all possible symmetries. No peak splitting characteristic of structural phase transitions was observed in our temperature-dependent measurements using both x rays and neutrons. In order to account for any resolution limited satellite reflection the full width half maximum (FWHM) of all reflections was studied using a Lorentzian profile. The extracted FWHM of selected reflections between 10 and 400 K [indicated in Fig. 1(a) by $R_1 \equiv (3\,1\,0)$ in $Pm\bar{3}m$ or {(1 3 4),(1 2 8)} in $R\bar{3}c$ or {(1 1 6), (3 3 2), (4 2 0)} in $I4/mcm$ or {(0 6 4), (2 6 0), (0 2 12), (2 0 12), (6 2 0), (6 0 4)} in $Imma$ and $R_2 \equiv (3\,1\,1)$ in $Pm\bar{3}m$ or {(0 4 2), (2 2 6), (0 2 10)} in $R\bar{3}c$ or {(4 2 2), (2 0 6)} in $I4/mcm$ or {(2 6 4), (2 2 12), (6 2 4)} in $Imma$] are shown in to Fig. 1(b). The FWHM of all the examined reflections which are supposed to split broadens upon cooling below ~300 K. This is not the case for $R_0 \equiv (1\,0\,0)$ in $Pm\bar{3}m$ or $(0\,1\,2)$ in $R\bar{3}c$ which shows temperature-independent FWHM. Although the observation of temperature-dependent FWHM in some particular reflections might indicate a departure from cubic symmetry, new reflections were not observed in our diffractogram. The diffraction data were further refined with FULLPROF[27] using the Rietveld method. A typical refinement, with $R_{wp} = 8.3\%$, is shown in Fig. 1(a). The inset to Fig. 1(a) shows the extracted lattice parameter in cubic symmetry vs temperature. The extracted lattice parameter is in excellent agreement with reference data.[7] Linear thermal expansion is observed between 100 and 300 K. The calculated volume thermal-expansion coefficient α_V after fitting the lattice parameter with a linear function normalized to the lattice parameter at 300 K is $\alpha_V = 9.9(1) \times 10^{-6}$ K^{-1}.

Minor deviations from linearity are observed between 200 and 270 K which might support the claim of instabilities in this region. However, no sign for a phase transition is observed.

The neutron-diffraction data obtained at POWGEN were further refined with JANA2006[28] using the Rietveld method resulting in $R_{wp} = 7.4\%$. The extracted lattice parameter in cubic symmetry is in excellent agreement with the one extracted using x rays. In addition, the atomic displacement parameters (ADPs) of Eu, Ti, and O at 180 K extracted in the harmonic approximation are 21.0(8), 7.3(5), and 7.5(5)($\times 10^{-3}$ Å^2) respectively and do not show any substantial irregularity vs temperature. Note that in isostructural $SrTiO_3$ the atomic displacements of Sr and Ti in the antiferrodistortive phase are comparable[29] to that of Eu in $EuTiO_3$.

Typical Mössbauer spectra between 90 and 325 K are given in Fig. 2. The data were fitted with a two-component model, the second component contributing by less than 1(1)% to the total area. The extracted isomer shift for the major component is −12.45(5) mm/s relative to EuF_3, an isomer shift indicative of Eu(II). Thus, the sample contained purely divalent Eu. The upper limit of Eu(III) which might escape detection is 1%. A Debye temperature of 295(5) K was calculated within

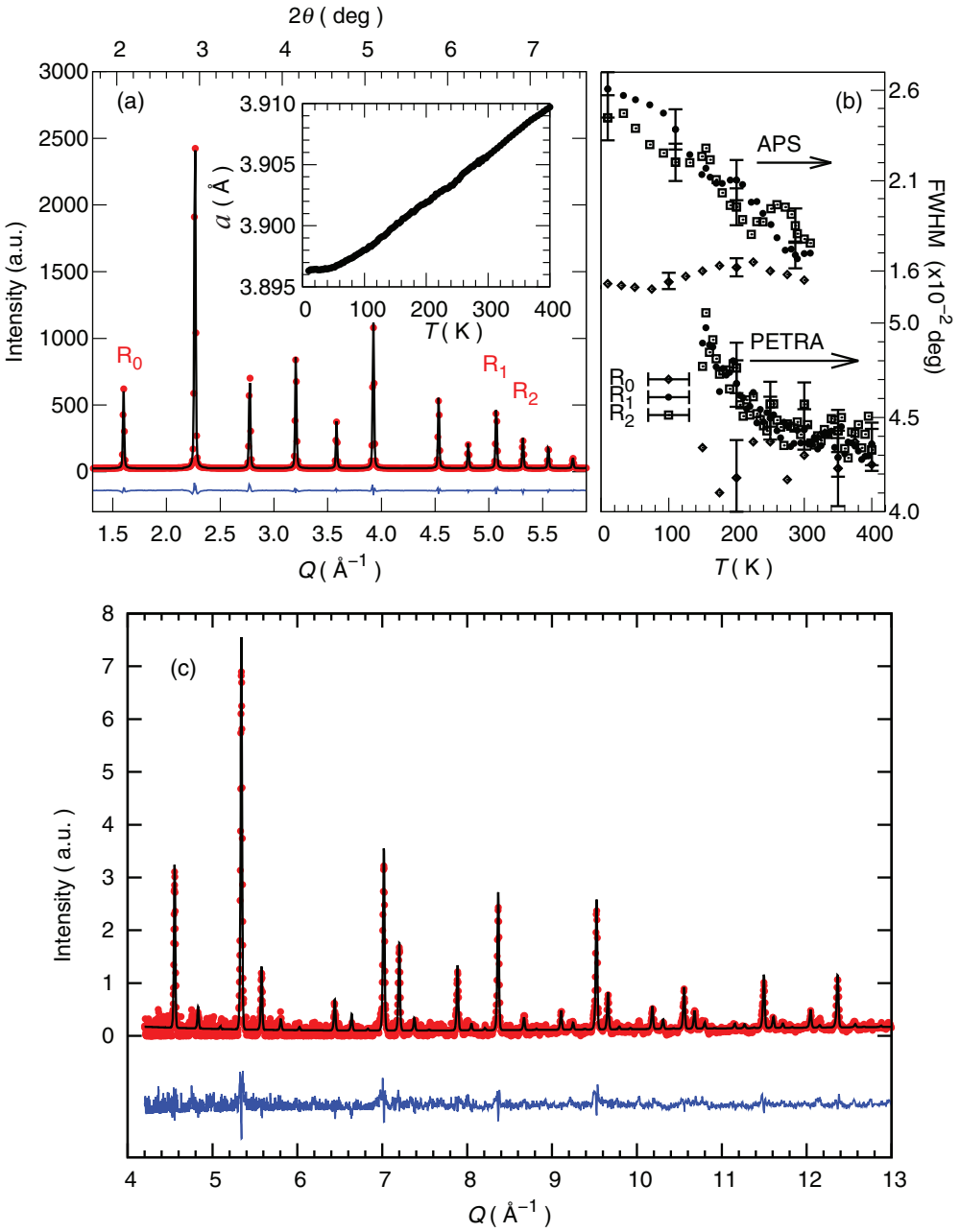

FIG. 1. (Color online) Rietveld refinement (black line) of a typical $EuTiO_3$ diffractogram (red points) and the corresponding refinement residuals (blue line) using (a) synchrotron radiation at 300 K and (c) neutrons at 180 K. (b) The FWHM of certain reflections (R_0, R_1, and R_2) measured with two different instrumental resolutions (see text). Inset to (a) shows the temperature-dependent lattice parameter (point size defines error bars) in cubic symmetry.

the Debye approximation[30] from the temperature-dependent Lamb-Mössbauer factor f_{LM}. In contrast to the prediction by Bussmann-Holder *et al.*[8] no line splitting or broadening was found in our temperature-dependent Mössbauer spectra.

Pair distribution function analysis (PDF) probes local disorder in crystalline materials.[31,32] In contrast to Rietveld refinements, the diffuse scattering and other background contributions are of crucial importance because a Fourier transformation is applied to the total scattering function. In this case, the large neutron absorption combined with the time-of-flight instrument prevents accurate background subtraction and produces oscillations in the extracted PDF thus in this study background contributions are treated phenomenologically. The refinement was conducted using PDFGUI[33] between 2.5 and 50 Å; see Fig. 3(a). Within the limited precision of our extracted PDF no clear change with temperature in the interatomic distances of oxygen with Europium is observed; see Fig. 3(b).

Several experimental methods for probing lattice dynamics exist. However, access to the full density of phonon states (DPS), $g(E)$, is feasible only by inelastic neutron[34] or x-ray scattering.[35] In this work, nuclear resonance inelastic measurements which require the existence of Mössbauer active isotope and synchrotron radiation were carried out. The raw

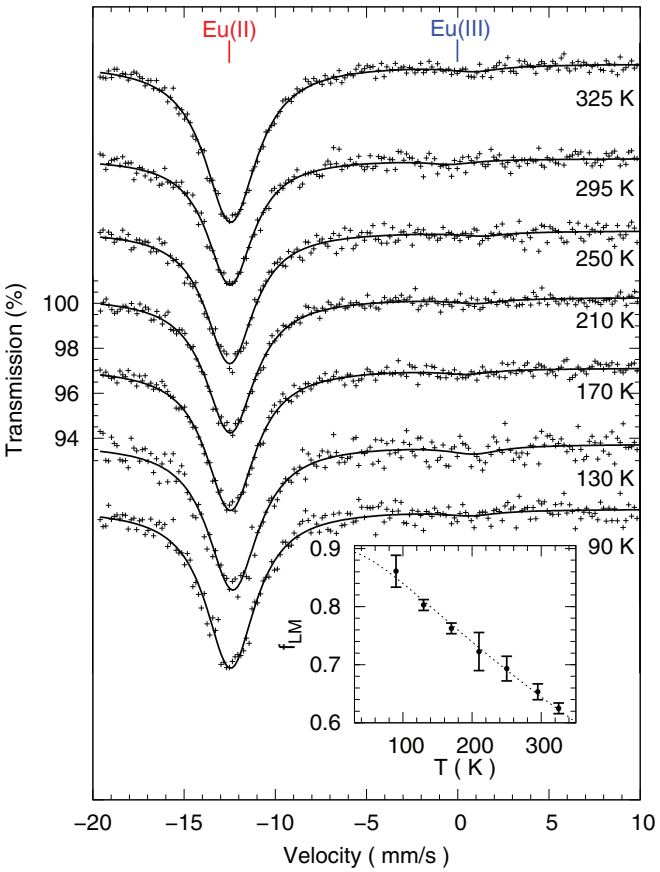

FIG. 2. (Color online) Temperature-dependent ^{151}Eu-Mossbauer spectra measured on $EuTiO_3$ powder (black points) and the corresponding two component model (black line). The expected isomer shift relative to EuF_3 is indicated with tics. The inset shows the temperature-dependent Lamb-Mössbauer factor f_{LM} of the majority phase, Eu(II), extracted from the spectra and the associated Debye model (black dashed line).

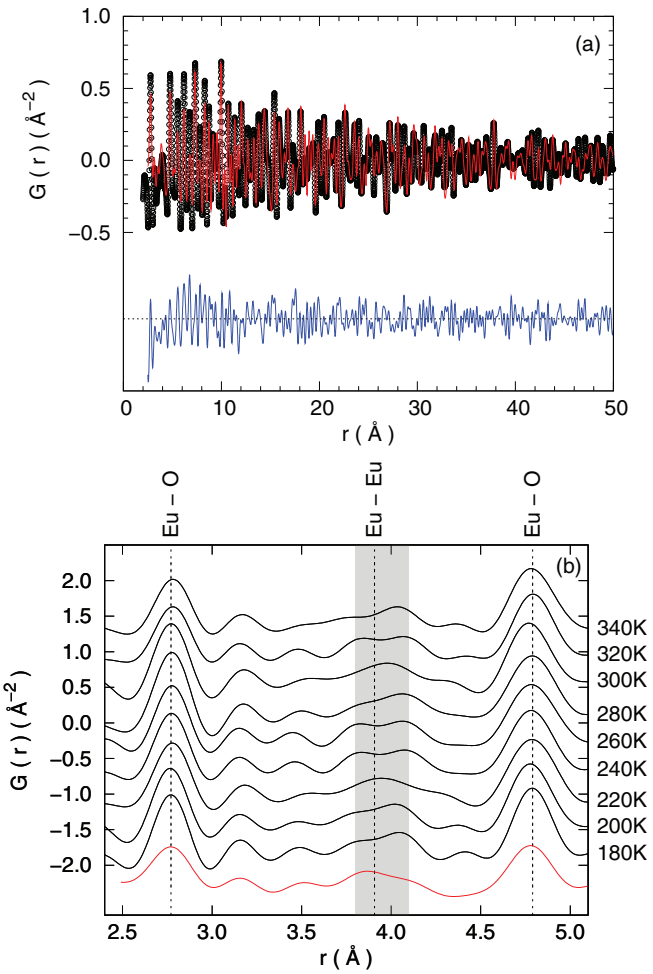

FIG. 3. (Color online) (a) Pair distribution function analysis (PDF) of neutron-scattering data, $Q = 50$ Å (black points), at 300 K, and the corresponding refinement (red line). The refinement residual (blue line) is given in the same scale and represents a fair refinement. (b) A close up in the temperature-dependent PDF analysis (black lines) and a typical PDF analysis refinement (red line) around the first nearest-neighbor distances regime, indicated with dashed lines. Note that at a lattice parameter distance, 3.905 Å at room temperature (RT), Ti-Ti and O-O pair correlations coexist with Eu-Eu.

spectra were treated using a modified version[36] of the program DOS.[37] The ^{151}Eu-specific density of phonon states (DPS)[38] was extracted between 0 and 24 meV; see Fig. 4(a). A single peak around 11.5 meV is observed, in agreement with our first-principles calculations in all possible symmetries. No resolvable change has been observed in the ^{151}Eu DPS between 210 and 360 K. The ^{151}Eu mean force constant can be extracted from our data using the expression $\langle F_i \rangle = M_i \int_0^\infty g(E) E^2 dE/\hbar^2$, where M_i is the mass of the resonant isotope. Between 110 and 360 K the extracted ^{151}Eu mean force constant ranges 78–70 N/m. From our NIS data the Eu ADP, $\langle u^2 \rangle$, were extracted using $\langle u^2 \rangle = -\ln f_{LM}/k^2$, where k is the wave number of the resonant photons. $\langle u^2 \rangle$ are in fair agreement with these extracted from neutron diffraction due to incoherent-coherent origin, respectively.[39] In the long-wavelength limit, in this work assumed below 4 meV, the average speed of sound, v_s, can be extracted from the DPS using: $\lim_{E\to 0} \frac{g(E)}{E^2} = \frac{M_i}{2\pi\hbar^3 \rho v_s^3}$ (Ref. 40) where M_i is the isotopic mass and ρ is the mass density. A linear fit of the $g(E)/E^2$, below 4 meV, between 110 and 360 K is given in Fig. 4(c). The extracted speed of sound is included in the same figure.

B. Macroscopic characterization

In order to verify claims of a *striking* phase transition observed in the heat capacity C_p of $EuTiO_3$,[8,41] the same cryostat, Quantum Design, was used. Special attention was taken on the thermal coupling between the measuring platform and the sample.[42] Every data point was measured three times and an average value has been extracted. The averaged data are shown in Fig. 4(b). The measured heat capacity in $EuTiO_3$ reveals no evidence of a structural phase transition in contrast with what has been observed in Refs. 8 and 41 and using similar techniques in $SrTiO_3$.[43] Hence, we conclude that the observation reported in Refs. 8 and 41 is related either to sample purity or inadequate background subtraction.

The isotropic elastic tensors C_{11} and C_{44}, were extracted from the spectrum of resonant ultrasound spectroscopy and the bulk, $B_{295\,K} = 125$ GPa, and shear, $G_{295\,K} = 76$ GPa, moduli were calculated. The extracted polycrystal shear wave speed

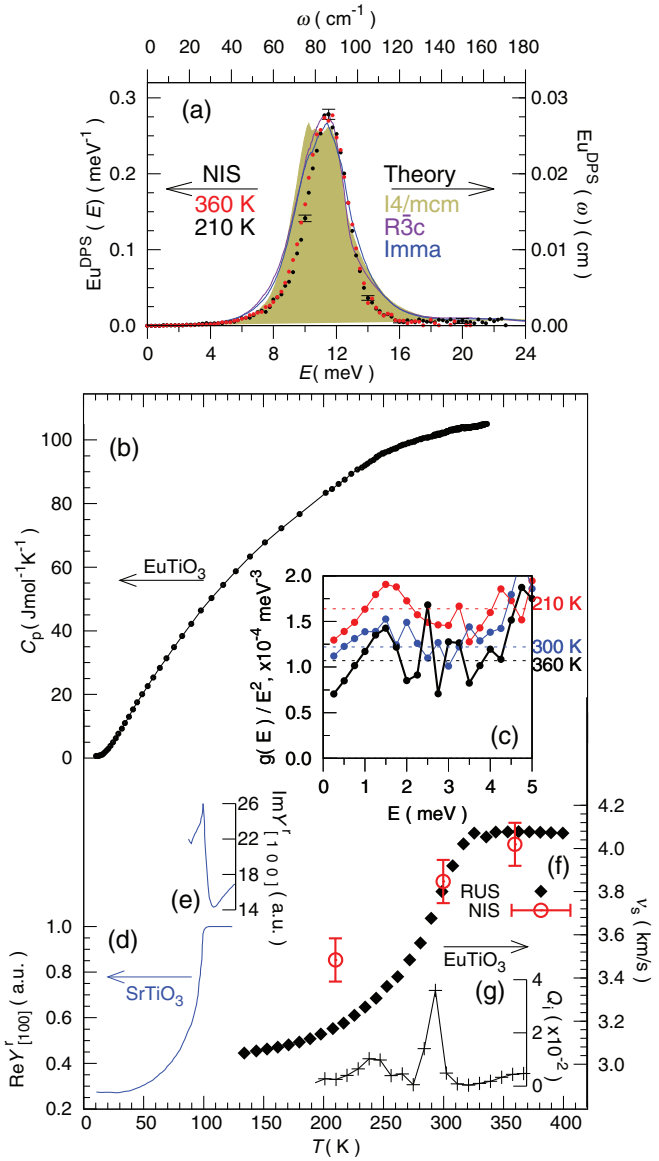

FIG. 4. (Color online) (a) The Eu specific density of phonon states in $EuTiO_3$ at 210 K (black tics) and 360 K (red line-tics) measured using NIS, typical errorbar is given, and our theoretical spectra for different structures.[26] (b) Heat capacity data between 10 and 340 K measured on $EuTiO_3$ using calorimetry (pointsize defines errorbar), line between points is guide to the eye. (c) The first 5 meV of the reduced ^{151}Eu projected density of phonon states, $g(E)/E^2$, and the related Debye levels (dashed lines). (d) The real part, $\mathrm{Re}Y^r_{[100]}$, and the imaginary part, (e), $\mathrm{Im}Y^r_{[100]}$, of the complex Young's modulus in $SrTiO_3$ obtained from Ref. 45. (f) Speed of sound extracted from RUS (black points), pointsize defines errorbar, and the corresponding extracted from NIS (red circles) at 210, 300 and 360 K. (g) The inverse quality factor of the resonance at 590 kHz between 200 and 370 K.

v_s is shown in Fig. 4(f). In Fig. 4(g) the inverse quality factor, Q_i,[44] of a typical mechanical resonance at 590 kHz is shown. The average speed of sound calculated from the isotropic elastic tensor indicates 25% hardening at 300 K relative to 100 K. Similar behavior was observed on a second sample from the same batch.

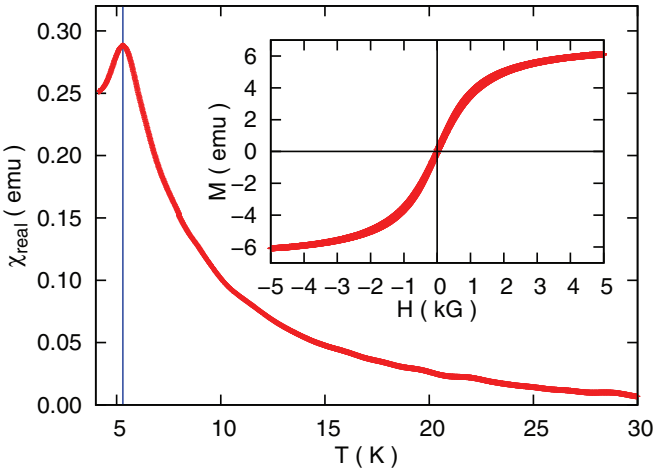

FIG. 5. (Color online) Temperature dependence of the ac magnetic susceptibility measured on cooling in sample in $EuTiO_3$ using an oscillating magnetic field with frequency $f = 20.4$ Hz, amplitude $H_{ac} = 10$ G, at $H_{dc} = 0$ G. Inset shows a M-H curve measured on the same sample at 4.9 K with maximum applied magnetic field of $H_{dc} = 50$ kG.

In our magnetic characterization measurements, see Fig. 5, a prominent peak at $T = 5.2(1)$ K appears in magnetic susceptibility. No other magnetic transitions were identified below 30 K. Below the observed transition, at 4.9 K, dc magnetization was measured up to $\mu_0 H_{dc} = 5$ T and neither a hysteretical behavior nor a ferromagnetic contribution were observed.

C. Theoretical investigations

Our first-principles calculations[26] on $EuTiO_3$ show that the $Pm\bar{3}m$ symmetry is unstable at the M and R points of the Brillouin zone with respect to the rotation of the oxygen octahedra. The lattice instabilities are removed when the structure relaxes in one of three symmetries: tetragonal ($I4/mcm$), orthorhombic ($Imma$), or rhombohedral ($R\bar{3}c$) all with relative relaxation energies between -25 and -27 meV to the cubic symmetry. The energy difference between the distorted structures is very small and allows in fact polymorphism. The Eu specific density of phonon states in all calculated structures is in excellent agreement with the measured one; see Fig. 4(a). We note that in the $Imma$ phase a Eu atomic displacement is allowed and its calculated size[26] is 0.012 Å.

IV. DISCUSSION

Although no obvious structural instability was identified by diffraction or calorimetry, a prominent acoustical stiffening upon heating is nevertheless observed between 100 and 300 K, a stiffening which is coroborated by a peak in the quality factor Q_i at 290 K. In the same temperature range the diffraction peaks which are supposed to split upon phase transition broaden on cooling; see Fig. 1. Above 310 K the FWHM of the same reflections as well as the speed of sound are found to be essentially temperature independent. A similar behavior was observed in the real and imaginary part of Young's modulus around 100 K in $SrTiO_3$,[45] see Figs. 4(d) and 4(e), however, in

$SrTiO_3$ a well-known structural transition around 100 K takes place.[46] Based on ultrasonic experiments Rehwald[47] qualifies the observed phase transition in $SrTiO_3$ as a second order and not as order-disorder but as soft mode type. In order to understand the nature of the acoustical stiffening in $EuTiO_3$ which appears rather similar to the one observed in $SrTiO_3$ detailed structural and phase purity analysis was carried out.

Divalent Eu based titanium compounds, such as $EuTiO_3$, have been investigated extensively by McGuire *et al.*[48] owing to their remarkable variety in magnetic properties. Among them, pyrochlore compound $Eu_3Ti_2O_7$ and Eu_2TiO_4 perovskite are impurity candidates in any $EuTiO_3$ sample. According to literature,[49] both compounds show ferromagnetic transitions around 8.7 ± 0.3 K. However, in our magnetization data, see Fig. 5, neither ferromagnetic transition appeared around 9 K nor is a ferromagnetic contribution present in the M-H curve below the antifferomagnetic transition temperature. As a result, within our instrumental resolution and with the combined use of several characterization methods, neither $Eu_3Ti_2O_7$ nor Eu_2TiO_4 are present in our sample. Thus combining the results of magnetic characterization with the Mössbauer spectroscopy our sample properties are consistent with the reported antiferromagnetic properties of $EuTiO_3$,[49] and preclude other Europium titanates.[50–52]

Mössbauer spectroscopy and nuclear inelastic spectroscopy are complementary methods since they are based on the same principle. This is illustrated once more by the fact that the NIS extracted f_{LM} agrees within 95% with the one extracted by Mössbauer spectroscopy. From the long-wavelength limit, below 4 meV, of the DPS the speed of sound v_s was calculated. The DPS extracted speed of sound indicates hardening of $EuTiO_3$ versus temperature, as observed also using RUS; see Fig. 4(f). Both microscopic and macroscopic measurements are in good agreement. The 10% deviation at 210 K is reproducible and can be associated with isothermal speed of sound measured via scattering, and adiabatic sound measured with RUS. As a result, the increase in speed of sound upon heating is verified both by microscopic and macroscopic techniques and is in contrast to the usual softening of elastic constants upon heating[53] confirming lattice instability of $EuTiO_3$ between 100 and 300 K. The temperature behavior of the adiabatic speed of sound is not consistent with an order-disorder transition.[47]

Pair distribution function analysis (PDF) probes local disorder in crystalline materials.[31,32] The PDF can be derived either from x-ray or neutron total scattering data with advantages and disadvantages described extensively by Egami and Billinge.[20] In this study we carried out PDF analysis on our neutron data because if there was any potential oxygen displacement it would be more visible using neutrons due to the enhanced neutron cross section with respect to x rays. The main information extracted from PDF without further modeling is the interatomic distances; see Fig. 3(b). Ti has a negative coherent scattering length which results in negative peaks for the A,X-Ti correlations, where A and X are the perovskite sites. Europium neutron absorption introduces anomalous background in the total scattering as function of the scattering angle. Hence, the Fourier transformation of the total scattering function might introduce artifacts in the PDF which cannot be modeled. Figure 3(a) shows the room-temperature PDF of $EuTiO_3$. Although all interatomic distances were modelled successfully and the extracted parameters (lattice parameters, atomic displacement parameters) agree with those extracted from Rietveld refinement, the goodness of fit is relatively poor. In case there was a pronounced phase transition, the interatomic distance between Eu-Eu, Ti-Ti, and O-O would change and a doublet instead of single peak is expected at the corresponding interatomic distance. However, the highlighted part of Fig. 3(b) does not show any consistent variation. The expected Eu-Eu correlation peak, and similarly the Ti-Ti and O-O, is not observed probably because the variations in PDF introduced by Eu absorption was not modelled correctly.

TABLE I. Temperature-dependent anharmonic refined parameters $D_{GC}^{ijkl}(r)$ of Eu atom in $EuTiO_3$ refined using the Gram-Charlier expansion.

	Temperature (K)			
$i,j = 1,2,3$	320	295	250	180
$D_{GC}^{iiii}(r)$	−426.0(1)	−375.6(1)	−329.8(1)	−88.7(1)
$D_{GC}^{iiij}(r)$	−65.7(8)	−67.5(6)	−69.2(7)	−35.1(4)

Although absolute values of ADPs extracted using coherent techniques such as diffraction might be affected by occupancies, relative changes of the ADPs extracted from such measurements are still valid. Although all extracted ADPs have smooth dependence on temperature the Eu ADP is large as compared to Ti and O; see Fig. 6(a). Hence, a Fourier map study in the vicinity of Eu was carried out. The Gram-Charlier expansion of anharmonic atomic displacement parameters is extensively described in Ref. 54 and has been followed in several cases of perovskite structure[55,56] with reported anharmonic atomic displacements. In this study, the Eu atomic displacement parameters extracted from neutron diffraction assuming cubic symmetry, $Pm\bar{3}m$, was modeled using a Gram-Charlier expansion of the probability density function (p.d.f.), p_{Eu}^{GC}, up to fourth-rank tensor[57] given in Eq. (1):

$$p_{Eu}^{GC}(r) = p_{Eu}^{harm}(r)\left(1 + \frac{1}{4!}D_{GC}^{ijkl}(r)H_{ijkl}(r)\right), \qquad (1)$$

where r is the atomic displacement vector relative to the equilibrium position, $H_{ijkl}(r)$ is the Hermite polynomial of fourth order, and $D_{GC}^{ijkl}(r)$ are anharmonic refined parameters [the third-order cumulants, $C_{GC}^{ijkl}(r)$ are zero, based on the site symmetry]. The use of a fourth-order Gram-Charlier expansion[54] for the Eu ADP improves the refinement. A reduction of the reliability factor from 5.03% to 4.07% just by adding a single parameter $D_{GC}^{1111}(r)$ has been observed. The refined Eu anharmonic parameters $D_{GC}^{ijkl}(r)$ at 110, 210, 295, and 360 K are given in Table I. Indeed, the Gram-Charlier tensor is following the symmetry restriction and therefore for the Eu at (0,0,0); $C_{GC}^{ijkl}(r)$ are zero and $D_{GC}^{ijkl}(r)$ are nonzero only for $D_{GC}^{1111}(r) = D_{GC}^{2222}(r) = D_{GC}^{3333}(r)$ and $D_{GC}^{1122}(r) = D_{GC}^{1133}(r) = D_{GC}^{2233}(r)$. To justify the existence of such anharmonic behavior on the Eu site similar treatment has been attempted on the Ti and O sites. No major refinement improvement has been observed and thus we have no evidence for strong anharmonic behavior on the Ti and O sites. In Fig. 6(b) the Europium p.d.f. after final refinement at 180 K is illustrated. Eu exhibits

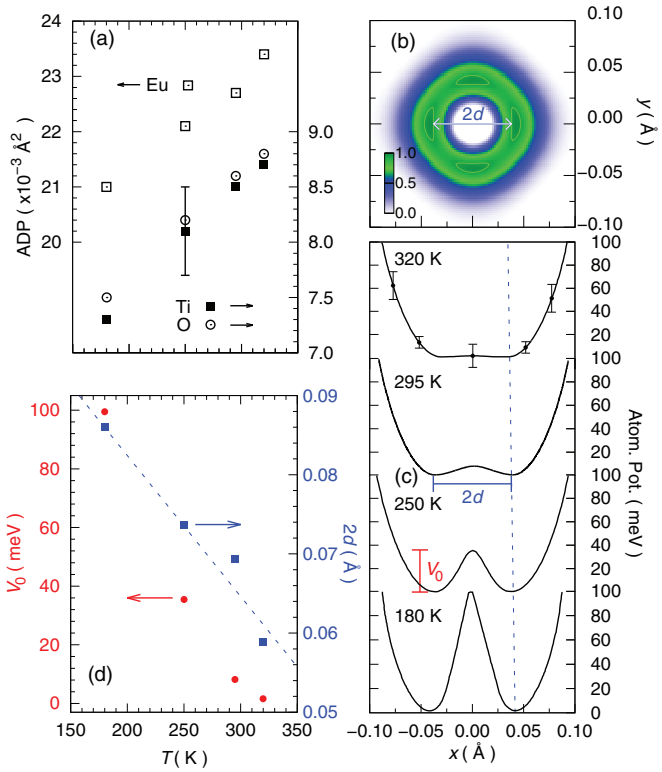

FIG. 6. (Color online) (a) The atomic displacement parameters (ADPs) extracted in the harmonic approximation from neutron diffraction; typical error bar is given. (b) Probability density function (p.d.f.), distribution of the Eu atom in the *ab* plane at 180 K. (c) The effective one-particle potential of the Eu atom along the *a* direction ($y = 0$) at 320, 295, 250, and 180 K obtained from crystallographic structure analysis and the typical error bar. (d) The potential barrier V_0 and the displacement from equilibrium position $2d$ (dashed line is guide to the eye) extracted from the potential given in (c).

off-centering in [1 0 0] and [0 1 0] directions (and equivalently in the [0 0 1] direction) with significant residual probability density in the azimuthal direction. The effective one-particle atomic potential $V(r)$ is related to the p.d.f. by

$$V(r) = -k_B T \ln\left[p_{Eu}^{GC}(r)/p_{Eu}^{GC}(r_0)\right], \qquad (2)$$

where k_B is the Boltzmann constant and T is temperature. In Fig. 6 a section of the Eu one-particle potential extracted according to Eq. (2) is depicted along the [1 0 0] direction. These sections reveal that Eu exhibits temperature-dependent off-centering, see Fig. 6(d), with $d \sim 0.04$ Å at 180 K. In addition, the potential barrier along the azimuthal direction flattens well before 295 K, whereas at 250 K a double well potential is already formed. Note that this is the same temperature region in which specific diffraction peaks, see Fig. 1, start to broaden upon cooling. Above 295 K, the Eu p.d.f. forms a plateau. An analogous double-well potential for $EuTiO_3$ was suggested theoretically by Bettis *et al.*[14] although for oxygen displacement.

The plateau in the p.d.f. indicates increased Eu anharmonicity. In order to quantify anharmonicity, we estimated using our macroscopic measurements of C_p, α_V, B, and the Grüneisen rule[58] the Grüneisen parameter. Our estimation of γ at 290 K is 1.3(1) in the same range with typical metallic compounds, $\gamma \simeq 2$. To elucidate the impact of the Grüneisen parameter on our measured DPS we used the vibrational frequency definition of the Grüneisen parameter, $\gamma = -\frac{d\ln E}{d\ln V}$, which relates the change in phonon mode energy to the change in volume. The estimated phonon mode energy shift between 110 and 360 K using our measured $\frac{dV}{V} \sim 0.0025$ and our extracted average Grüneisen parameter of $\gamma = 1.3$ results in $\frac{\delta E}{E} \sim 0.004$. Therefore, the prominent peak around 11 meV will not shift due to anharmonicity by more than 0.04 meV. Such energy mode shift is currently resolution limited.

$EuTiO_3$ is an incipient ferroelectric, which means that its lattice is close to a ferroelectric instability at low temperatures. Note that theoretical calculations[26] indicate that the Eu displacement from its high-symmetry position is possible in tilted structures, e.g., *Imma*, however, this displacement is static. Significant dynamical displacement of Eu was observed in cubic $Pm\bar{3}m$ structure even for the low-energy optical mode TO1, which eigenvector constitutes 37% of the Last mode and 60% of the Slater; see Ref. 26. This observation was used to design ferroelectric (Eu,Ba)TiO_3 ceramics with significant off-centering on the magnetic cation site.[59] Also magnetoelectric coupling in $EuTiO_3$ is exceptionally high[60] due to strong contribution of magnetic Eu cation in the low-energy polar mode. Note that in other multifferroics nonmagnetic ions are displaced, e.g., Bi in $BiFeO_3$ or Y in $YMnO_3$, therefore the magnetoelectric coupling is usually smaller in such materials. Microscopic origin of the mixing character of the low-energy polar mode in cubic $EuTiO_3$ is the coupling of the $4f$ orbitals of Eu^{2+} with the $3d$ states of nonmagnetic Ti^{4+}.[61] The influence of this coupling on the lattice instabilities of $EuTiO_3$ was recently studied by Birol and Fennie.[62] It was found that partial occupation of the d states on Ti due to hybridization drives $EuTiO_3$ away from ferroelectric instability. This conclusion is compatible with results of Ref. 26, where it was shown that increasing volume of cubic $EuTiO_3$, i.e., decreasing f-d hybridization, turns the low-energy mode unstable, with Slater-type atomic displacement. Nevertheless, it is still not clear what is the effect of the oxygen vacancy on the structural stability of $EuTiO_3$. Recently, it was shown[63] that doping $EuTiO_3$ by N favors the tilted *Pnma* structure also at high temperatures. By means of hybrid functional calculations of electronic structure it was shown that the presence of impurities as well as the tilting of oxygen octahedra lead to delocalization of the Eu f states, which modifies f-d coupling between A and B sites and, therefore, changes the lattice stability conditions. Note that *Pnma* is subgroup of the *Imma* considered in Ref. 26, and is the one with off-centered Eu position. Thus, this particular field is still open to research and further theoretical and experimental studies are yet to come which will clarify the microscopic origin of the observed Eu shift in $EuTiO_3$.

The lattice dynamics in $EuTiO_3$ resembles that of $SrTiO_3$, the atomic delocalization in phase change materials,[64] as well as the lattice dynamics in PbTe.[65,66] In such cases the associated potential energy is considered as a multivalley surface with drastic impact on thermal conductivity.[67] The observed phenomenon resembles rattling between minima in the potential energy and could be harnessed to lower the lattice thermal conductivity.

V. CONCLUSION

In summary, the combination of the extracted speed of sound by RUS and NIS, the Gram-Charlier expansion of Eu atomic displacements based on neutron diffraction and the feedback from theoretical studies based on *ab initio* calculations provides evidence for Europium delocalization which originate in lattice instabilities in the system. Short-range coexistence of crystallographic phases with candidate symmetries $Imma$, $R\bar{3}m$, and $I4/mcm$ in $EuTiO_3$ might be related to the fact that Eu delocalization does not lead to a structural transition. Experimental studies under high pressure on phase pure $EuTiO_3$ single crystals or thermal diffuse scattering experiments using synchrotron radiation might shed further light on this scenario. In addition, according to theoretical calculations a Eu atomic displacement is allowed in the $Imma$ phase and its calculated size,[26] 0.012 Å, corresponds roughly to the one measured in our experiment, however, a phase transition with long-range order is not observed. Reasonable scenarios might be nucleation of nanoclusters with $Imma$ symmetry and a different distortion direction which fail to extend to a reasonable correlation length or dynamical fluctuation of the distortion. Measurements of acoustic emission as it was presented[68] on $BaTiO_3$ might clarify this scenario. Similar atomic off-centering has been observed in a series of ferroelectric compounds such as $Pb(Zr,Ti)O_3$ and $Pb(Mg_{1/3}Nb_{2/3})O_3$.[69]

ACKNOWLEDGMENTS

The Helmholtz Association of German research centers is acknowledged for funding (VH NG-407 "Lattice dynamics in emerging functional materials" and VH NG-409 "Computational Nanoferronics Laboratory"). The European Synchrotron Radiation Facility, the Advanced Photon Source, the PETRAIII, and the Spallation Neutron Source are acknowledged for provision of synchrotron radiation and neutron beam time at ID22N, 6-ID-D, P02.1, POWGEN, and NOMAD, respectively. The work in the Czech Republic has been supported by the Czech Science Foundation (Project No. P204/12/1163), MEYS (LD 11035 and LD 12026 - COST MP0904), and the ERDF (CEITEC - CZ.1.05/1.1.00/02.0068). We are grateful to Dr. D. Robinson, Dr. M. Feygenson, and Dr. J. Neuefeind for help during data acquisition and Jülich Supercomputing Center for support.

*Present address: European Synchrotron Radiation Facility, F-38043 Grenoble, France.
†Present address: Los Alamos National Laboratory, Los Alamos, New Mexico 87545, USA.
‡Present address: Deutsches Electronen-Synchrotron, D-22607 Hamburg, Germany.
§r.hermann@fz-juelich.de

[1] C. Li, K. C. K. Soh, and P. Wu, J. Alloys Compd. **372**, 40 (2004).
[2] H. D. Zhou and J. B. Goodenough, J. Phys. Condens. Matter **17**, 7395 (2005).
[3] A. M. Glazer, Acta Crystallogr., Sect. B **28**, 3384 (1972).
[4] T. R. McGuire, M. W. Shafer, R. J. Joenk, H. A. Alperin, and S. J. Pickart, J. Phys. Condens. Matter **37**, 981 (1966).
[5] T. Katsufuji and H. Takagi, Phys. Rev. B **64**, 054415 (2001).
[6] J. H. Lee *et al.*, Nature (London) **466**, 954 (2010).
[7] J. Brous, I. Fankuchen, and E. Banks, Acta Crystallogr. **6**, 67 (1953).
[8] A. Bussmann-Holder, J. Köhler, R. K. Kremer, and J. M. Law, Phys. Rev. B **83**, 212102 (2011).
[9] M. Allieta, M. Scavini, L. J. Spalek, V. Scagnoli, H. C. Walker, C. Panagopoulos, S. S. Saxena, T. Katsufuji, and C. Mazzoli, Phys. Rev. B **85**, 184107 (2012).
[10] J. Köhler, R. Dinnebier, and A. Bussmann-Holder, Phase Transit. **85**, 949 (2012).
[11] J.-W. Kim, P. Thompson, S. Brown, P. S. Normile, J. A. Schlueter, A. Shkabko, A. Weidenkaff, and P. J. Ryan, Phys. Rev. Lett. **110**, 027201 (2013).
[12] V. Goian, S. Kamba, O. Pacherová, J. Drahokoupil, L. Palatinus, M. Dušek, J. Rohlíček, M. Savinov, F. Laufek, W. Schranz *et al.*, Phys. Rev. B **86**, 054112 (2012).
[13] D. S. Ellis, H. Uchiyama, S. Tsutsui, K. Sugimoto, K. Kato, D. Ishikawa, and A. Q. R. Baron, Phys. Rev. B **86**, 220301 (2012).
[14] J. L. Bettis, M.-H. Whangbo, J. Köhler, A. Bussmann-Holder, and A. R. Bishop, Phys. Rev. B **84**, 184114 (2011).
[15] I. P. Swainson, C. Stock, P. M. Gehring, G. Xu, K. Hirota, Y. Qiu, H. Luo, X. Zhao, J.-F. Li, and D. Viehland, Phys. Rev. B **79**, 224301 (2009).
[16] M. Kachlik, K. Maca, V. Goian, and S. Kamba, Mater. Lett. **74**, 16 (2012).
[17] M. Ross and J. S. Story, Rep. Prog. Phys. **12**, 291 (1949).
[18] A. Huq, J. Hodges, L. Huke, and O. Gourdon, Z. Kristallogr. Proc. **1**, 127 (2011).
[19] J. C. R. H. J. Neuefeind, M. Feygenson, and K. K. Chipley, Nucl. Instrum. Methods Phys. Res. B **287**, 68 (2012).
[20] T. Egami and S. J. L. Billinge, *Underneath the Bragg Peaks: Structural Analysis of Complex Materials* (Pergamon, New York, 2003).
[21] A. Migliori, J. Sarrao, W. M. Visscher, T. Bell, M. Lei, Z. Fisk, and R. Leisure, Physica B **183**, 1 (1993).
[22] E. Alp, W. Sturhahn, T. Toellner, J. Zhao, M. Hu, and D. Brown, Hyperfine Interact. **144–145**, 3 (2002).
[23] R. Rüffer and A. Chumakov, Hyperfine Interact. **97–98**, 589 (1996).
[24] O. Leupold, J. Pollmann, E. Gerdau, H. D. Rüter, G. Faigel, M. Tegze, G. Bortel, R. Rüffer, A. I. Chumakov, and A. Q. R. Baron, Europhys. Lett. **35**, 671 (1996).
[25] D. Alfè, Comput. Phys. Commun. **180**, 2622 (2009).
[26] K. Z. Rushchanskii, N. A. Spaldin, and M. Lezaic, Phys. Rev. B **85**, 104109 (2012).
[27] J. Rodríguez-Carvajal, Physica B **192**, 55 (1993).
[28] V. Petříček, M. Dušek, and L. Palatinus, JANA2006. *The Crystallographic Computing System* (Institute of Physics, Praha, Czech Republic, 2006).
[29] M. Kopecký, J. Fábry, and J. Kub, J. Appl. Crystallogr. **45**, 393 (2012).

[30]R. H. Herber, *Chemical Mössbauer Spectroscopy* (Plenum, New York, 1984).
[31]X. Qiu, T. Proffen, J. F. Mitchell, and S. J. L. Billinge, Phys. Rev. Lett. **94**, 177203 (2005).
[32]I.-K. Jeong, T. W. Darling, J. K. Lee, T. Proffen, R. H. Heffner, J. S. Park, K. S. Hong, W. Dmowski, and T. Egami, Phys. Rev. Lett. **94**, 147602 (2005).
[33]C. L. Farrow, P. Juhas, J. W. Liu, D. Bryndin, E. S. Boin, J. Bloch, T. Proffen, and S. J. L. Billinge, J. Phys. Condens. Matter **19**, 335219 (2007).
[34]M. Christensen, N. Lock, J. Overgaard, and B. B. Iversen, J. Am. Chem. Soc. **128**, 15657 (2006).
[35]E. Burkel, Rep. Prog. Phys. **63**, 171 (2000).
[36]The DOS program was modified for reconvoluting the extracted DPS with a Gaussian function with the same FWHM as the measured instrumental function.
[37]V. Kohn and A. Chumakov, Hyperfine Interact. **125**, 205 (2000).
[38]The natural abundance of ^{151}Eu is 47.8% and no further isotopic enrichment was needed.
[39]B. C. Sales *et al.*, *Semiconductors and Semimetals* (Academic, New York, 2001).
[40]N. W. Ashcroft and N. D. Mermin, *Solid State Physics* (Brooks/Cole, Belmont, MA, 1976).
[41]A. P. Petrović, Y. Kato, S. S. Sunku, T. Ito, P. Sengupta, L. Spalek, M. Shimuta, T. Katsufuji, C. D. Batista, S. S. Saxena *et al.*, Phys. Rev. B **87**, 064103 (2013).
[42]QD-PPMS, *Heat Capacity Application Note 1085-152 A* (Quantum Design, Inc, San Diego, CA, 2002).
[43]M. C. Gallardo, R. Burriel, F. J. Romero, F. J. Gutiérrez, and E. K. H. Salje, J. Phys. Condens. Matter **14**, 1881 (2002).
[44]The inverse quality factor quantifies the dampness of an oscillator.
[45]A. V. Kityk, W. Schranz, P. Sondergeld, D. Havlik, E. K. H. Salje, and J. F. Scott, Europhys. Lett. **50**, 41 (2000).
[46]F. W. Lytle, J. Appl. Phys. **35**, 2212 (1964).
[47]W. Rehwald, Adv. Phys. **22**, 721 (1973).
[48]T. R. McGuire, B. E. Argyle, M. W. Shafer, and J. S. Smart, J. Appl. Phys. **34**, 1345 (1963).
[49]J. E. Greedan and McCarthy, Mater. Res. Bull. **7**, 531 (1972).
[50]N. L. Henderson, J. Baek, P. S. Halasyamani, and R. E. Schaak, Chem. Mater. **19**, 1883 (2007).
[51]K. Syamala, G. Panneerselvam, G. Subramanian, and M. Antony, Thermochim. Acta **475**, 76 (2008).
[52]G. McCarthy, W. White, and R. Roy, J. Inorg. Nucl. Chem. **31**, 329 (1969).
[53]Y. P. Varshni, Phys. Rev. B **2**, 3952 (1970).
[54]W. F. Kuhs, Acta Crystallogr., Sect. A: Found. Crystallogr. **48**, 80 (1992).
[55]B. Etschmann, N. Ishizawa, V. Streltsov, and S. Oishi, Z. Kristallogr. **216**, 455 (2001).
[56]E. A. Zhurova, Y. Ivanov, V. Zavodnik, and V. Tsirelson, Acta Crystallogr., Sect. B: Struct. Sci. **56**, 594 (2000).
[57]*International Tables for Crystallography* (International Union of Crystallography, Chester, England, 1995).
[58]E. S. R. Gopal, *Specific Heats at Low Temperatures* (Heywood, London, 1966).
[59]K. Rushchanskii, S. Kamba, V. Goian, P. Vaněk, M. Savinov, J. Prokleška, D. Nuzhnyy, K. Knížek, F. Laufek, S. Eckel *et al.*, Nat. Mater. **9**, 649 (2010).
[60]V. V. Shvartsman, P. Borisov, W. Kleemann, S. Kamba, and T. Katsufuji, Phys. Rev. B **81**, 064426 (2010).
[61]H. Akamatsu, Y. Kumagai, F. Oba, K. Fujita, H. Murakami, K. Tanaka, and I. Tanaka, Phys. Rev. B **83**, 214421 (2011).
[62]T. Birol and C. J. Fennie, Phys. Rev. B **88**, 094103 (2013).
[63]L. Sagarna, K. Z. Rushchanskii, A. Maegli, S. Yoon, S. Populoh, A. Shkabko, S. Pokrant, M. Lezaic, R. Waser, and A. Weidenkaff, J. Appl. Phys. **114**, 033701 (2013).
[64]T. Matsunaga, N. Yamada, R. Kojima, S. Shamoto, M. Sato, H. Tanida, T. Uruga, S. Kohara, M. Takata, P. Zalden *et al.*, Adv. Funct. Mater. **21**, 2232 (2011).
[65]K. M. O. Jensen, E. S. Bozin, C. D. Malliakas, M. B. Stone, M. D. Lumsden, M. G. Kanatzidis, S. M. Shapiro, and S. J. L. Billinge, Phys. Rev. B **86**, 085313 (2012).
[66]E. S. Božin, C. D. Malliakas, P. Souvatzis, T. Proffen, N. A. Spaldin, M. G. Kanatzidis, and S. J. L. Billinge, Science **330**, 1660 (2010).
[67]M. Christensen, S. Johnsen, and B. B. Iversen, Dalton Trans. **39**, 978 (2010).
[68]E. Dul'kin, J. Petzelt, S. Kamba, E. Mojaev, and M. Roth, Appl. Phys. Lett. **97**, 032903 (2010).
[69]T. Egami, in *Ferro- and Antiferroelectricity*, edited by N. Dalal and A. Bussmann-Holder, Vol. 124 (Springer, Heidelberg, 2007), pp. 69–88.